Journal of Catalysis 271 (2010) 170–177

Contents lists available at ScienceDirect

Journal of Catalysis

journal homepage: www.elsevier.com/locate/jcat

# Nitroaldol reactions catalyzed by amine-MCM-41 hybrids

Qingqing Wang, Daniel F. Shantz *

*Artie McFerrin Department of Chemical Engineering, Texas A&M University, College Station, TX 77843-3122, United States*

ARTICLE INFO

*Article history:*
Received 9 July 2009
Revised 4 January 2010
Accepted 7 January 2010
Available online 24 February 2010

*Keywords:*
MCM-41
Nitroaldol reaction
Surface-tethered amines

ABSTRACT

The catalytic properties of several amine-functionalized MCM-41 materials in the nitroaldol (Henry) reaction are reported. The work investigated the effects of organoamine type (primary, secondary, tertiary), amine density, and the presence of silanol groups on the catalytic activity and product selectivity. High selectivity to the nitroalcohol product was achieved by introducing secondary and tertiary amine groups on the MCM-41 surface, while the nitroalkene is the dominant product for primary amines. Steric effects appear to be significant in determining the overall reactivity as the least sterically hindered amines are the most active. The capping of silanols with trimethylsilyl groups resulted in a reduction in catalytic activity for nearly all samples, indicating the importance of surface silanols and/or the surface polarity in the reaction.



## 1. Introduction

During the past decade, ordered mesoporous silicas (OMS) have been intensely studied as catalysts, catalyst supports, adsorbents, and as containers for cluster/nanowire growth [1–11]. While it was originally hoped that mesoporous silicas would represent large-pore analogs of zeolites (i.e. high acidity and thermal stability), this has not come to pass. However, based on their well-ordered structure, high surface area and tunable pore diameters, OMS materials have emerged as model supports for investigating a wide range of homogenous catalysts tethered to solid supports [12–16].

The academic community has spent significant effort over the last several years investigating the catalytic properties of organic groups covalently attached to mesoporous silica [10,17–21]. While thiol and sulfonic acid groups have been attached to MCM-41 and SBA-15 [18,22–24], the bulk of the works have investigated the properties of amines attached to OMS. Researchers have focused on two respects in order to improve the reactivity and stability of amine–OMS catalysts. First, many investigations showed that the reactivity of hybrid catalysts is indeed dependent on the dispersion and accessibility of functional sites that can be influenced by the support structure [25–30], density or isolation of organic groups [22,31–37], and the immobilization procedure [8,35,38–43]. The second was tuning the functionality based on the targeted reactions or designing multi-functional catalysts. Different simple amine groups were covalently attached to OMS by bulk imprinting, co-condensation, or post-synthetic grafting methods [44]. Brunel and co-workers compared the catalytic activities of primary amino or tertiary amino groups attached MCM-41 in the Knoevenagel condensation [19]. Bigi et al. [30] indicated that the activity scale of supported amines strongly parallels that of the corresponding homogeneous counterparts, the order of amine activity being primary > secondary > tertiary in nitroaldol condensation at 90 °C. Lin and co-workers showed that the base strength has positive effects on the rate of the reaction [45,46]. Kitayama and co-workers showed FSM-16 functionalized with secondary amines is more active for the aldol reaction [47,48] than FSM-16 functionalized with primary amines. Katz and co-workers [49,50] found that acid–base cooperativity between surface silanols and primary amines also affects chemical reactivity and that the cooperativity favored the selectivity to unsaturated products in base-catalyzed reactions, such as the Michael, Henry, and Knoevenagel reactions. Asefa and co-workers [51] have shown the product selectivity in the Henry reaction changes if the reaction is catalyzed by secondary or tertiary amine groups attached MCM-41 [52]. Several groups have explained their results with respect to the catalytic mechanisms based on the physical and chemical properties of functional groups on OMS surface, like the imine and ion-pair mechanisms indicated by Katz and co-workers [50] and Asefa and co-workers [52] as well as nucleophilic/elctrophile theory used by Brunel [20] and Lin and co-workers [53].

Labs have also investigated the synthesis of materials containing multiple functional groups. Brunel and co-workers [54] introduced a non-functional group of phenyl silane to dilute the density of the grafted aniline as the functional group. That works suggests that the activity of aniline groups is a linear function of their number density. Work from Davis's laboratory [55–58] has reported materials containing both sulfonic acid and amine groups as well as materials containing primary amine groups with carboxylic acid groups on SBA-15. Higher conversion in the aldol reaction

* Corresponding author. Fax: +1 979 845 6446.
*E-mail address:* Shantz@chemail.tamu.edu (D.F. Shantz).

0021-9517/$ - see front matter © 2010 Elsevier Inc. All rights reserved.
doi:10.1016/j.jcat.2010.01.010

was obtained when weaker acid components were combined in these base–acid catalysts. Lin's group synthesized base–acid-functionalized mesoporous silica nanospheres. Their results indicate the cooperativity of the electrophile and nucleophile enhanced the reaction rates of the aldol and nitroaldol reactions [23,53,59,60]. Some cooperative action of acid–base, acid–thiol, amine–urea in OMS materials, especially the effect of bifunctionality and the functional group spatial arrangement, have been summarized by Margelefsky et al. [61].

This report summarizes our efforts in characterizing the reactivity of amines supported on ordered mesoporous silica for the Henry reaction. In the current report, three aspects of this problem are investigated in detail, the chemical nature of the amine, the effect of surface silanol groups, and how the identity of the silica substrate impacts reactivity.

## 2. Experimental

### 2.1. General

Sodium silicate (PQ Brand N, $SiO_2$ 28.7%, $SiO_2/Na_2O$ = 3.22), cetyltrimethylammonium bromide (CTAB, Fisher Chemical, high purity grade), sulfuric acid ($H_2SO_4$, Sigma–Aldrich, 95–98% A.C.S reagent), sodium hydroxide (NaOH, Mallinckrodt Chemicals, pellet), methanol (Fisher Chemical, 99%), tetraethoxysilane (TEOS, ⩾99%, Fluka), Pluronic P123 ($EO_{20}PO_{70}EO_{20}$, MW = 5800, BASF), and hydrochloric acid (HCl, Sigma–Aldrich, reagent grade, 37%) were used as received. The following compounds, also used as received, were used in the post-synthetic grafting: 3-(aminopropyl)triethoxysilane (APTES, 99%, Sigma–Aldrich), chloropropyltriethoxysilane (TCI America, ⩾97% (GC)), benzyl bromide (TCI America, ⩾98% (GC)), methylamine hydrochloride (Alfa Aesar, ⩾98%), piperazine (Fluka, ⩾98%), diisopropylethylamine (DIPEA, 99%, Alfa Aesar), and hexamethyldisilazane (HMDS, Fluka, ⩾98% (GC)). Hexane (EMD Chemicals Inc., ⩾95%), toluene (Sigma–Aldrich, ⩾99.5%), and tetrahydrofuran (THF, Sigma–Aldrich, ⩾99%) were dried using an MBraun solvent purification system. Deuterated chloroform ($CDCl_3$, D, 99.8% + 1%V/V TMS, CIL Inc.) was used as the solvent for the $^1H$ NMR measurements.

### 2.2. OMS synthesis

MCM-41 was synthesized using the reported procedure of Edler and White [62]. SBA-15 samples were synthesized using the method reported by Zhao et al. [63]. As an example for the synthesis of MCM-41, 7.9 g of sodium silicate solution were mixed with 45.4 mL deionized water. To the solution, 0.27 g of NaOH were added and then 7.8 mL of 1 M $H_2SO_4$ were added. To this solution, 7.29 g of CTAB were added, and the resulting mixture was stirred for 15 min at room temperature. The mixture was then placed in an oven at 100 °C for 24 h under static conditions. After 24 h, the sample was removed from the oven, allowed to cool sufficiently that it could be easily handled and titrated to pH = 10 using 1 M $H_2SO_4$. The sample was then placed back in the oven at 100 °C. The titration step was performed two additional times in regular 24-h intervals. The total heating period was 96 h. For the SBA-15 synthesis, 4.0 g of Pluronic P123 were dissolved in 60 mL of 4 M HCl and 85 mL of deionized water by stirring for 5 h at room temperature. Then, 8.5 g of TEOS were added to that solution and stirred for 24 h at 35 °C. The mixture was then aged at 80 °C for 24 h without stirring. After the synthesis period, the solid products were filtered, washed with deionized water, and air-dried overnight. The solid products were calcined to remove CTAB or Pluronic. The calcination procedure was as follows: the air-dried samples were heated from room temperature to 100 °C at a rate of 1 °C/min; held at 100 °C for 2 h; increased from 100 to 500 °C at a rate of 1 °C/min; and then held at 500 °C for 8 h.

### 2.3. Functionalization of OMS

The syntheses for generating the functionalized OMS materials are shown in Scheme 1. To generate the amine- and chloro-functionalized OMS materials, one gram of calcined MCM-41 was placed in a round-bottom flask and dried at 100 °C under vacuum for 1 h. Upon cooling, 100 mL of anhydrous toluene under nitrogen was added into the flask. An aliquot of APTES (46 μL (0.2 mmol), 92 μL (0.4 mmol), 184 μL (0.8 mmol)) or chloropropyltriethoxysilane (48 μL (0.2 mmol), 96 μL (0.4 mmol), 192 μL (0.8 mmol)) was added to the solution under argon. This mixture was stirred overnight at room temperature. The product was collected by filtration, washed with 50 mL of toluene, 50 mL of methanol, and 500 mL of deionized water sequentially and then air-dried. *N*-Methylpropylamine (**2**) and *N*,*N*-dimethylpropylamine (**5**) functionalized MCM-41 were prepared by adding *N*-(methylaminopropyl)trimethoxysilane (154 μL (0.8 mmol)) or *N*,*N*-(dimethylaminopropyl)trimethoxysilane (175 μL (0.8 mmol)) to substitute APTES in the procedure. Piperazine- and piperidine-functionalized MCM-41 were prepared from chloro-functionalized MCM-41. *1-Propyl piperazine MCM-41* (**3**) and *1-propyl piperidine MCM-41* (**6**). Forty-three milligrams of piperazine (0.5 mmol) or 40 μL (0.4 mmol) of piperidine and 1 mL of DIPEA (6 mmol) were added in 100 mL of THF, and stirred for 15 min. One gram of chloro-functionalized MCM-41 (0.8 mmol/g loading) was added into the solution. The mixture was stirred for 24 h at room temperature. The solid product was filtered, rinsed with 50 mL of THF, 200 mL of hexane, and 200 mL of methanol and air-dried. *N-propyl-N-benzylamine MCM-41* (**4**). For the synthesis of benzylpropylamine-functionalized MCM-41, one gram of amine-functionalized MCM-41 (0.8 mmol/g loading) was added into a flask with 100 mL of hexane with 175 μL (1 mmol) of DIPEA, and 119 μL (1 mmol) of benzyl bromide was added to the solution. The mixture was refluxed for 24 h. After the reaction, the sample was filtered, rinsed with 200 mL of hexane and 200 mL of ethanol and air-dried.

### 2.4. HMDS capping of the parent and functionalized MCM-41, and SBA-15

Samples were also made where the remaining silanols groups on the OMS surface were capped with hexamethyldisilazane (HMDS). A tube with one gram of functionalized OMS was evacuated on the Schlenk line under vacuum with heating for 1 h. Fifty milliliters of dry hexane were added to the sample under nitrogen. One gram (6.2 mmol) of HMDS was added into the tube under argon environment. The mixture in the closed container was stirred overnight. The product was filtered, rinsed with 200 mL of hexane and 200 mL of methanol and then air-dried. HMDS treated-samples are denoted as HMDS-**X**, where **X** refers to the number indicated in Scheme 1.

### 2.5. Analytical

Powder X-ray diffraction (PXRD) measurements were performed using a Bruker-AXS D8 powder diffractometer with Cu Kα radiation over a range of 0.8–10° 2$\theta$. Thermal gravimetric analyses (TGA) were performed using a TG 209C Iris instrument from Netzsch over a temperature range of 25–500 °C using oxygen and nitrogen as carrier gases and a temperature ramping rate of 2 °C/min. Nitrogen adsorption experiments were performed on a Micromeritics ASAP 2010 micropore system using approximately 0.06 g of sample. The samples were degassed under vacuum at room temperature for 2 h and then at 100 °C for 24 h before anal-

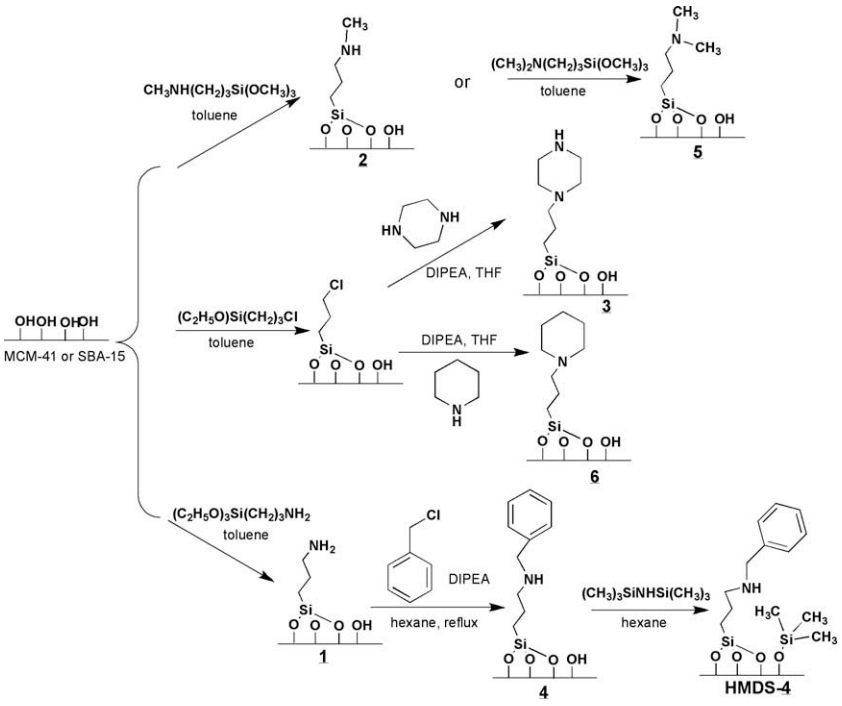


**Scheme 1.** Synthesis of OMS hybrids.

ysis. The mesopore volumes were determined using the $\alpha_s$-method [64,65]. The mesopore size distributions were calculated from the adsorption branch of the isotherms using the Barret–Joyner–Halenda (BJH) method with a modified equation for the statistical film thickness [66]. The reaction conversions and product identities were determined using solution $^1$H NMR. Spectra were acquired using a Mercury 300 spectrometer with a 30° pulse of 2 μs and a 3-s relaxation delay. The conversions and product selectivities were calculated by the intensity ratios of the peak $\delta$ = 5.58–5.64 ppm, $^1$H) due to the alcohol product 1-(4-nitrophenyl)-2-nitroethanol, the peak ($\delta$ = 7.6 ppm $^1$H) due to the unsaturated product, and the peak ($\delta$ = 9.9–10.1 ppm, $^1$H) due to nitrobenzaldehyde. Elemental analysis was performed by Galbraith laboratories.

### 2.6. Catalytic testing

The nitroaldol reaction (Henry reaction) was performed as follows: 100 mg of catalyst was loaded into a 10-mL Schlenk tube and heated in an oven 100 °C overnight. Upon cooling, 0.38 g (2.5 mmol) of nitrobenzaldehyde and 1.35 mL (25 mmol) of nitromethane were introduced into the tube. The mixture in the tube was kept at 40 °C while stirring. After different time intervals, 100 μL of the solution was transferred into a small glass tube, 1 mL of deuterated chloroform was added to the tube, and then the solid was removed from the solution using a centrifuge. The separated liquid was analyzed by $^1$H liquid NMR on a Mercury 300 spectrometer as described earlier. For the recycle studies, the solid was recovered by filtration, washed with nitromethane (2 mL, one time) and methanol (10 mL, 4 times), and dried at 100 °C for one day. Note that results are reported as mmol aldehyde consumed per mmol nitrogen per g silica. Given the variable amine loading employed and the fixed amount of aldehyde added in all reactions, the positions where these plots would plateau (corresponding to 100% conversion) is equal to 2.5 divided by the amine loading in mmol/g $SiO_2$. For completeness, the plots of conversion and selectivity versus time for all samples are included in the Supplementary Material. Also shown in the Supplementary Material is a plot of conversion versus time for **4**-MCM-41 where the plot shows multiple reaction runs to give an indication of reproducibility. On the basis of this plot and other comparable experiments on multiple samples, we believe the error on these measurements is less than ±5%.

## 3. Results and discussion

### 3.1. General characterization

Fig. 1 shows the powder X-ray diffraction patterns, adsorption isotherms, and BJH pore size distributions for the parent MCM-41, **1**-MCM-41, **4**-MCM-41 (0.8 mmol/g loading), and HMDS-**4**-MCM-41. The XRD results are consistent with literature results and indicate the target OMS phase is obtained. The nitrogen adsorption isotherms show that the mesopore volume and effective pore size decrease gradually with the increase in organic group loading. The isotherms of the other samples can be found elsewhere [67]. Table 1 shows the organic content as determined from thermal gravimetric analysis (TGA) and elemental analysis.

### 3.2. Catalytic testing

#### 3.2.1. Effect of amine loading and identity

All samples were investigated for the ability to catalyze the nitroaldol reaction. The parent (i.e. amine-free) MCM-41 silica is completely inert, and thus the catalytic activity observed is due to the amines attached on the OMS surface. Table 1 summarizes some of the key catalytic data, including the percent total conversion of the nitrobenzaldehyde, product selectivities and the turnover frequency (initial number of reaction events $h^{-1}$ amine site$^{-1}$) where the number of amines was estimated by elemental analysis and TGA. From Table 1, some general conclusions can be drawn. The propylamine sample (**1**) is the least active. That the secondary amines are more active is consistent with previous work [47,48]. Also consistent with previous literature, the product selectivity is dependent on the nature of the amine (i.e. primary versus

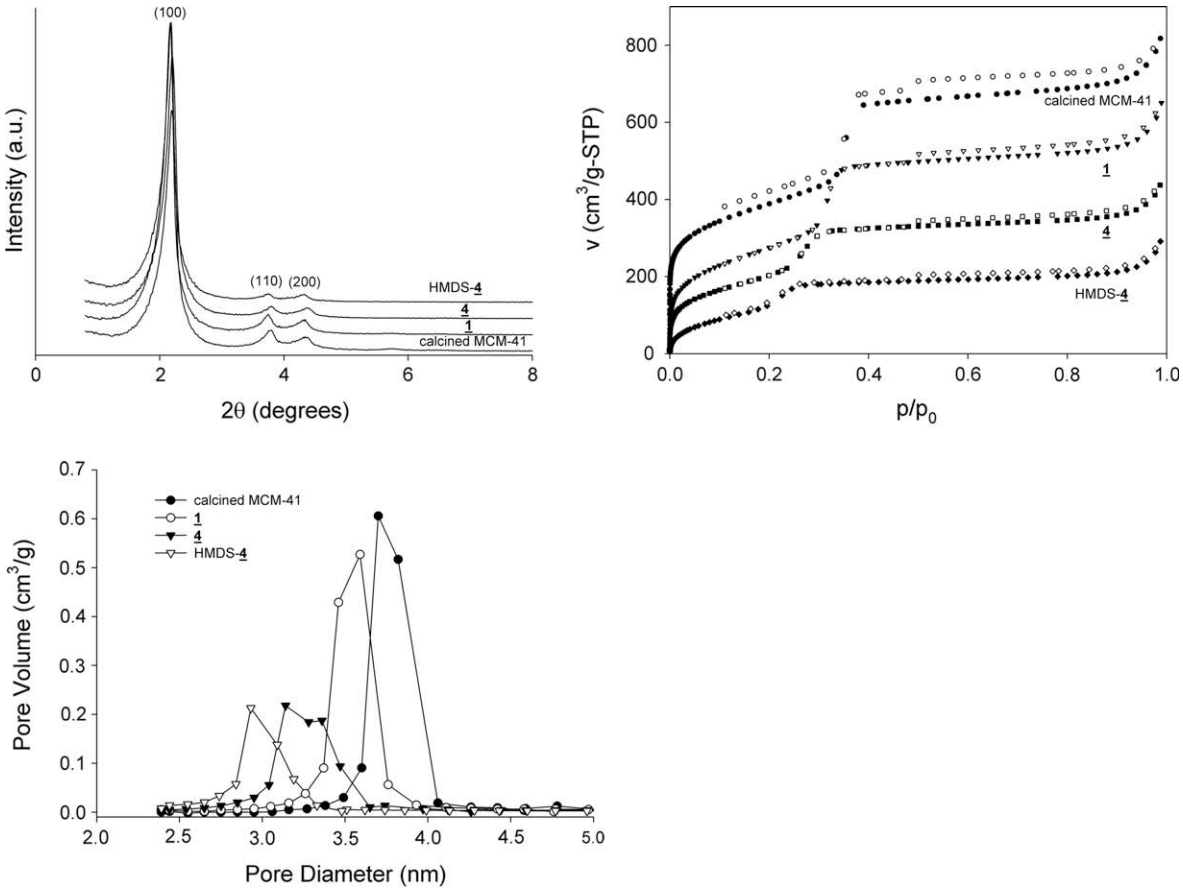


**Fig. 1.** (From top to bottom) Powder X-ray diffraction patterns, nitrogen adsorption isotherms, and BJH pore size distributions for MCM-41, **1**-MCM-41, **4**-MCM-41, and HMDS-**4**-MCM-41. The isotherm of MCM-41 has been shifted 100 $cm^3$/g-STP.

**Table 1**
Percent conversions at 1 h and 2 h, product selectivities, actual amine loadings (determined by TGA) and TOF values. Amine loadings in mmol/g.

| Sample ID | Time (h) | X (%) | $S_{OH}$ | $S_{=}$ | Amine loading | TOF ($h^{-1}$) |
|---|---|---|---|---|---|---|
| **1**-MCM-41-0.8 | 1 | 22 | 0.31 | 0.69 | 0.70 | 7.7 |
| | 2 | 45 | 0.31 | 0.69 | | |
| **1**-MCM-41-0.4 | 1 | 13 | 0.23 | 0.77 | 0.49 | 4.3 |
| | 2 | 22 | 0.38 | 0.62 | | |
| **2**-MCM-41-0.8 | 1 | 97 | 0.98 | 0.02 | 0.88 | 74.0 |
| **2**-MCM-41-0.2 | 1 | 54 | 0.9 | 0.1 | 0.31 | 50.3 |
| **3**-MCM-41-0.8 | 1 | 36 | 0.99 | 0.01 | 0.76 | 12.4 |
| | 2 | 56 | 0.98 | 0.02 | | |
| **3**-MCM-41-0.4 | 1 | 24 | 0.93 | 0.07 | 0.50 | 12.3 |
| | 2 | 37 | 0.92 | 0.08 | | |
| **3**-MCM-41-0.2 | 1 | 26 | 0.94 | 0.06 | 0.38 | 17.7 |
| | 2 | 41 | 0.94 | 0.06 | | |
| **4**-MCM-41-0.8 | 1 | 62 | 0.90 | 0.10 | 0.66 | 24.4 |
| | 2 | 89 | 0.85 | 0.15 | | |
| **4**-MCM-41-0.4 | 1 | 25 | 0.83 | 0.17 | 0.41 | 14.7 |
| | 2 | 44 | 0.80 | 0.20 | | |
| **4**-MCM-41-0.2 | 1 | 15 | 0.85 | 0.15 | 0.34 | 10.9 |
| | 2 | 31 | 0.82 | 0.18 | | |
| **5**-MCM-41-0.8 | 1 | 95 | 0.99 | 0.01 | 0.74 | 55.4 |
| | 2 | 98 | 0.99 | 0.01 | | |
| **6**-MCM-41-0.2 | 1 | 68 | 0.91 | 0.09 | 0.32 | 64 |
| | 2 | 86 | 0.93 | 0.07 | | |

secondary, tertiary). The primary amine sample (**1**) appears to follow the imine formation mechanism, which favors the nitrostyrene product, consistent with work by Bass et al. [50]. In contrast, the samples containing secondary amines give very high selectivities to the nitroalcohol product, between 0.8 and 0.9. Also noteworthy is that the selectivity to the nitroalcohol product increases with increasing amine loading. Finally, the selectivities also show differences that can likely be attributed to the structures of the different secondary amines, as will be discussed in detail in the following paragraphs. It is also important to note that the Supplementary Material contains plots of the selectivities versus time for all samples. We do not observe any significant interconversion of alcohol to alkene via dehydration or hydrolysis of alkene to alcohol. This conclusion is based on the observation that the selectivities are essentially constant during the reactions.

### 3.2.2. Effect of the amine identity

Fig. 2 shows the conversions and yields of the Henry reaction catalyzed by propylamine-functionalized MCM-41, **1**-MCM-41 sample. This is the one sample where the alkene product is dominant; the selectivity to the alcohol product is low (0.3). The TOF is low (7 h) relative to the other materials investigated. Previous literature reports of similar materials in the Henry reaction [50,52] at comparable reaction conditions give TOFs of 12 h with a selectivity to the alcohol product of 20%.

The results for **2**-MCM-41 are shown in Fig. 3. The differences between these samples and the simple propylamine-functionalized MCM-41 are striking. Both the activity and selectivity of this material are different. The conversions are much higher than for the samples of **1** and the selectivity is very high (>0.9) to the nitroalcohol product. The samples with target loadings of 0.8 mmol/g and 0.2 mmol/g give conversions of 97% and 57%, respectively, after 1 h. Note that the data shown in Fig. 3 for the high loading

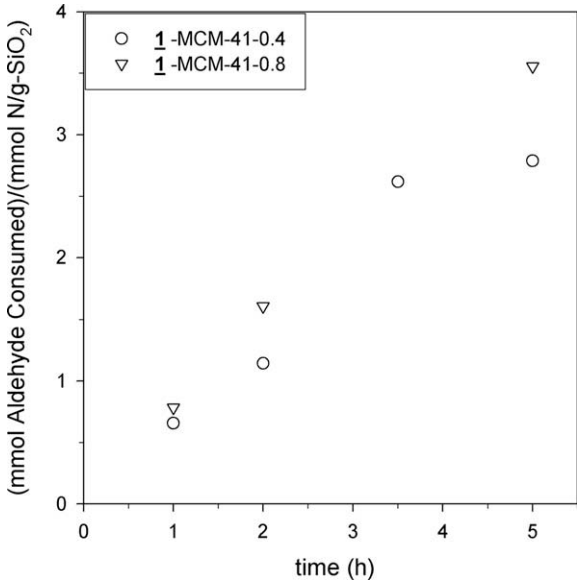


**Fig. 2.** Nitrobenzaldehyde consumption normalized by the mmol of nitrogen per gram of silica versus reaction time for **1**-MCM-41 as a function of amine loading.

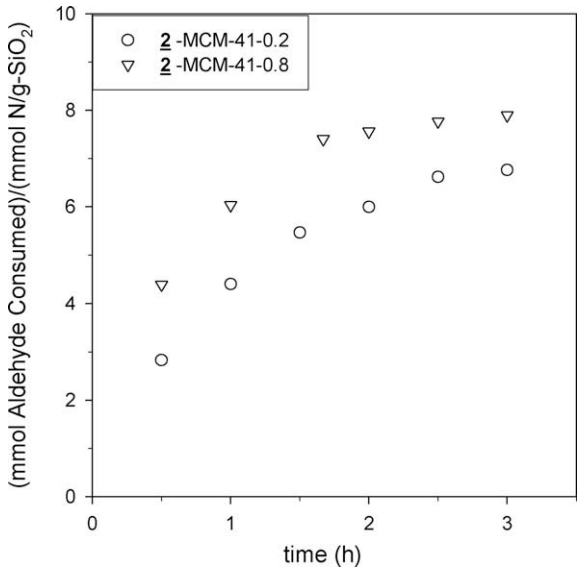


**Fig. 3.** Nitrobenzaldehyde consumption normalized by the mmol of nitrogen per gram of silica versus reaction time for **2**-MCM-41 as a function of amine loading. Note that for the high loading sample, 7.5 mmol of benzaldehyde was used instead of 2.5 mmol benzaldehyde.

sample used an initial amount of 7.5 mmol of benzaldehyde. The selectivity to alcohol product is over 90%. In order to calculate the initial TOF of the 0.8 mmol/g sample, three times the reactants described in Section 2 (i.e. 7.5 mmol of aldehyde) were used to measure conversions at short times. The TOFs (50 $h^{-1}$ and 74 $h^{-1}$ for 0.2 mmol/g and 0.8 mmol/g loading samples, respectively) shown in Table 1 indicate the **2**-MCM-41 samples have the largest reaction rate among the three secondary amine-functionalized MCM-41 samples. One explanation is that the methylpropylamine group facilitates the formation of an ion-pair, another that the least sterically hindered secondary amine should be the most active.

This result led us to explore other more sterically hindered secondary amines. Piperazine-functionalized MCM-41 samples (**3**-MCM-41) were also investigated. These materials (Fig. 4) displayed

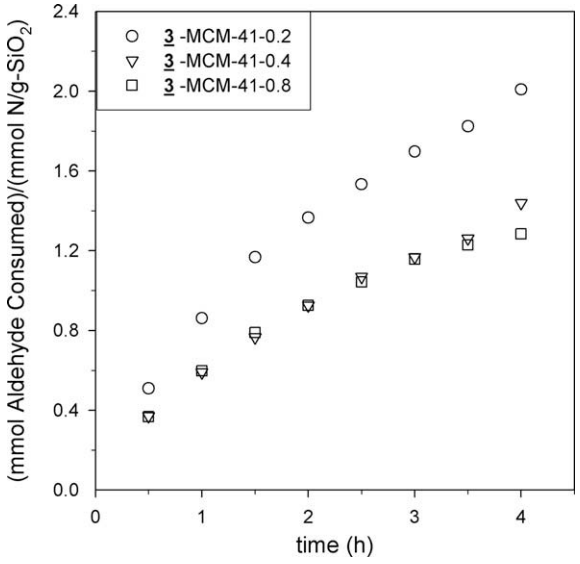


**Fig. 4.** Nitrobenzaldehyde consumption normalized by the mmol of nitrogen per gram of silica versus reaction time for **3**-MCM-41 as a function of amine loading.

an even higher selectivity to the alcohol, above 0.9 in all cases. It is also observed that with increased amine loading, the amount of nitroalkene formed decreases, going to essentially zero for the highest loading samples. In contrast to the previous two samples, here we clearly see that the lowest loading sample appears to have the highest activity on a per site basis. Consistent with that the TOF is largest for the lowest loading sample and the values are 17.7, 12.3, and 12.4 $h^{-1}$ for 0.38 mmol/g (0.2 target), 0.5 mmol/g (0.4 target), and 0.76 mmol/g (0.8 target) loading samples, respectively. One difference between this and the previous samples is that the steric bulk of this ligand is much larger. Related to this, the fact that the amine is in a more rigid cyclic structure may negatively impact its activity. Also, it is possible that at higher loading, there are more ligand–ligand interactions that lead to reduce activity. Clearly, the absolute activity of these samples is much lower than the methylamine samples (**2**). Initially, it was anticipated that the tertiary amine in the piperazine ring does not contribute to the observed activity due to steric effects. This was assessed directly based on ligand **6** discussed in the following paragraphs. We believe one explanation for the low amount of alkene formed is that the piperazine secondary amine is far enough from the surface that there are likely minimal interactions between it and the surface silanol groups. The low amount of alkene formed is also consistent with work from Asefa's laboratory [52].

Fig. 5 shows the conversions and product yields for the **4**-MCM-41 samples as a function of reaction time. As can be seen from Table 1, the nitroalcohol is the major product and the alcohol selectivity ranges from 0.7 to 0.9. Also, the conversion is seen to increase with increasing amine loading. At thirty minutes, the respective conversions are 7%, 13%, and 40% for **4** at loadings of 0.2, 0.4, and 0.8 meq/g, respectively. The 0.8 meq/g sample shows an approximately threefold increase in conversion compared to the 0.4 meq/g sample. For the **4**-MCM-41 samples, the TOF decreases from 24 $h^{-1}$ for 0.8 mmol/g, 15 $h^{-1}$ for 0.4 mmol/g, and 11 $h^{-1}$ for 0.2 mmol/g. That the TOF (initial number of reaction events $h^{-1}$ amine $site^{-1}$) is strongly dependent on the amine loading shows these do not behave as site-isolated materials. One explanation for the observed behavior is that there is cooperativity between the amines and/or silanol groups. In contrast to the other secondary amines, more alkene product is observed in this system. Also, the amount of alkene appears to increase slightly as the reac-

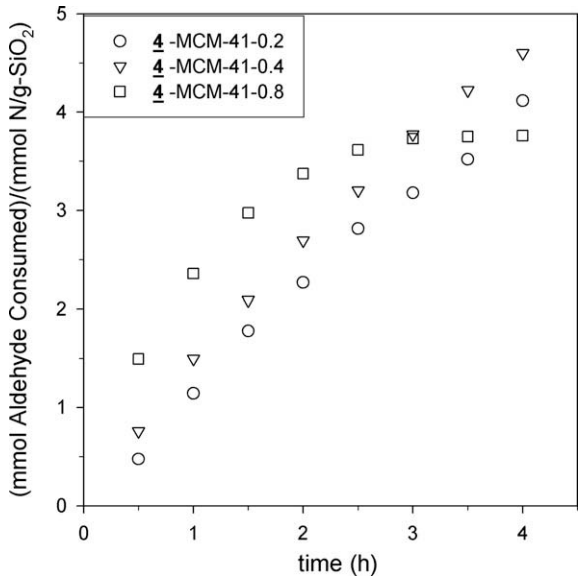


**Fig. 5.** Nitrobenzaldehyde consumption normalized by the mmol of nitrogen per gram of silica versus reaction time for **4**-MCM-41 as a function of amine loading.

tion proceeds, in contrast to the other two secondary amines investigated. This could be either due to stronger amine – surface silanol interactions in this system – or because the p*K* of the benzylamine should be lower than that of the methylamine and piperazine due to the substituent aromatic group.

Fig. 6 shows the consumption of benzaldehyde catalyzed by tertiary amine-functionalized MCM-41 samples. The **5**-MCM-41 sample (dimethylamine) shows similar conversions and product selectivities to that of **2**-MCM-41. After 1 h, the conversion is 96% and the selectivity to alcohol product is 0.99. The **6**-MCM-41 sample with 0.2 meq/g loading displays 65% conversion after 1 h, higher than that of the **3**-MCM-41 sample. The results indicate that the catalytic activity is dependent on the basic strength of the functional amine groups attached on MCM-41 as well as the steric structures surrounding the amines.

Based on the above-mentioned results, it would seem two key features affect the reactivity of the supported amines. The first is that non-cyclic amines appear to be more active than the cyclic amines. This is based on comparing the reactivity of the benzylamine and piperazine-functionalized silanes with the methyl and dimethylamine-functionalized silanes. It also appears that moving the amine farther from the surface has a negative effect on reactivity based on comparing the piperidine and piperazine substituted silanes.

### 3.2.3. Effect of hexamethyldisilazane capping

Previous work by Bass and co-workers [50,68] has shown that cooperativity by hydrogen bonding between the amine and silanol groups is possible in these materials. The above-mentioned work has also shown very clear differences in reactivity among several different secondary amines. To attempt to understand how the silanols affect the activity observed the samples discussed earlier were treated with hexamethyldisilazane (HMDS) to convert the surface silanol groups into trimethylsilyl moieties [68]. Fig. 7 shows the aldehyde consumption versus time for these materials. With the exception of the samples of **2**-0.8 capped with HMDS, all samples show a dramatic reduction in activity, with conversions below 20% in all cases. There are three ways this result can be interpreted. The first is that the high catalytic efficiency depends on the cooperative activation of reactants by the amines and the silanols. The second is that the bulk of the TMS fragment reduces access to the amine and thus suppresses reactivity. To probe this, a sample of **4** was treated with methyltrimethoxysilane, which should react with the silanol groups yet is much smaller. As can be seen in Fig. 8, the reaction rate is much lower upon capping with methyltrimethoxysilane and the conversion is linear with time. The calculated TOF decreases from 24.2 $h^{-1}$ to 6.3 $h^{-1}$. This result is certainly consistent with the first point mentioned earlier (cooperativity between silanols and amines). The third possibility is that capping the surface silanols made the materials so hydrophobic that the reagents would not adsorb into the material. This seems unlikely as the powders after HMDS capping still wet readily. One possible explanation for the high activity of **2**-0.8 capped with HMDS sample is that the silane chemistry is relatively incomplete. In order to check if that is the case, a sample of **2** with a lower amine loading (0.2 mmol/g) was capped with HMDS. After HMDS treatment, the conversion did decrease significantly, although the sample is still much more active than the other HMDS-capped

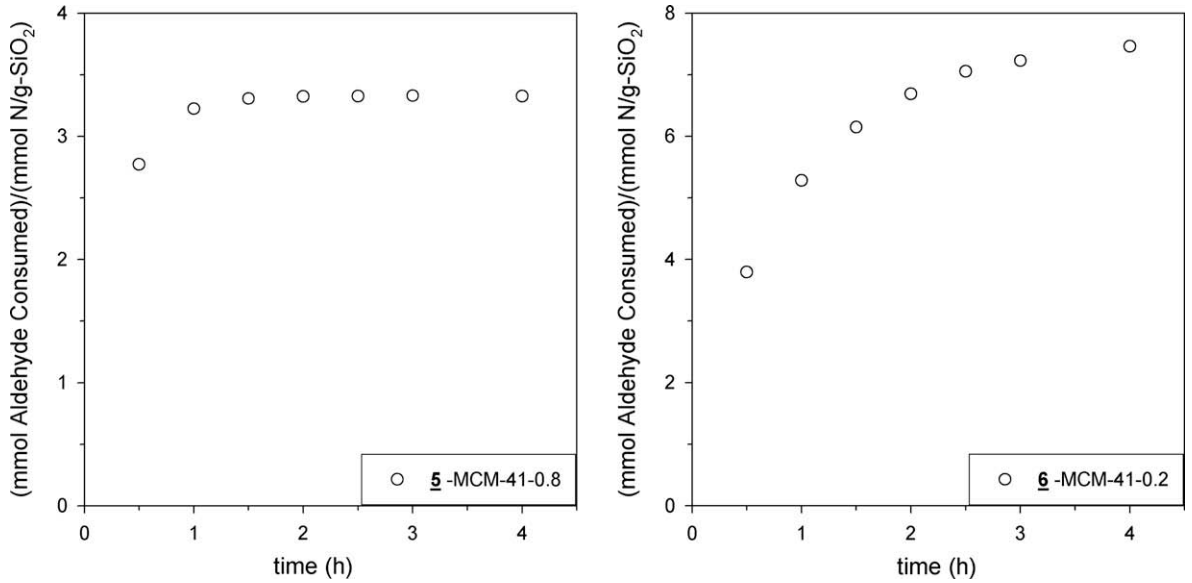


**Fig. 6.** Nitrobenzaldehyde consumption normalized by the mmol of nitrogen per gram of silica for **5**-MCM-41 with 0.8 meq/g loading (left) and **6**-MCM-41 with 0.2 meq/g loading (right).

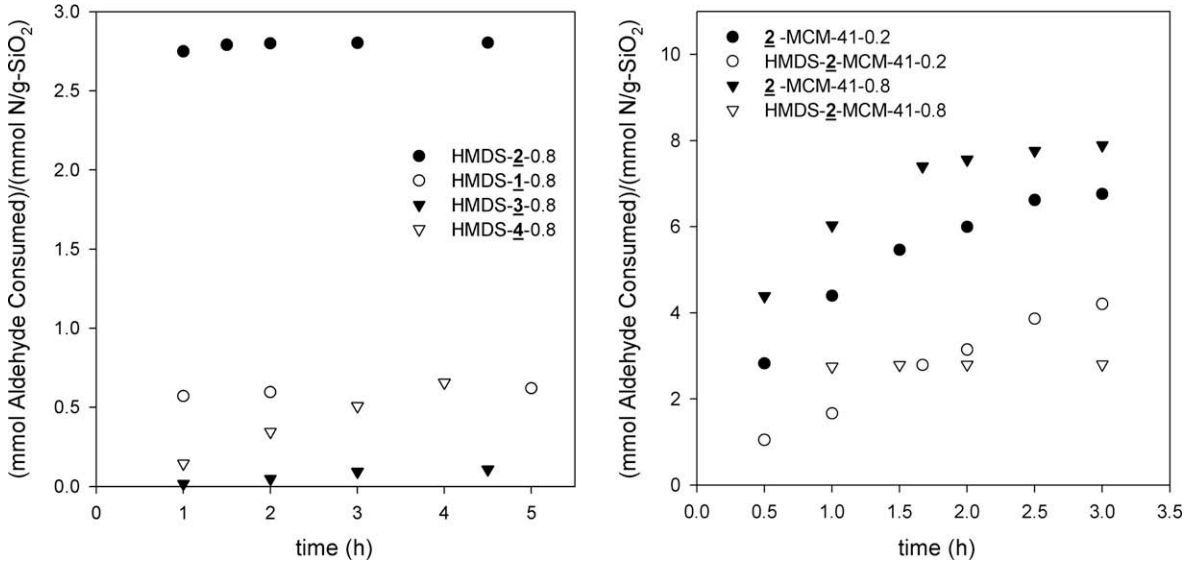


**Fig. 7.** Nitrobenzaldehyde consumption normalized by the mmol of nitrogen per gram of silica for several HMDS-capped samples.

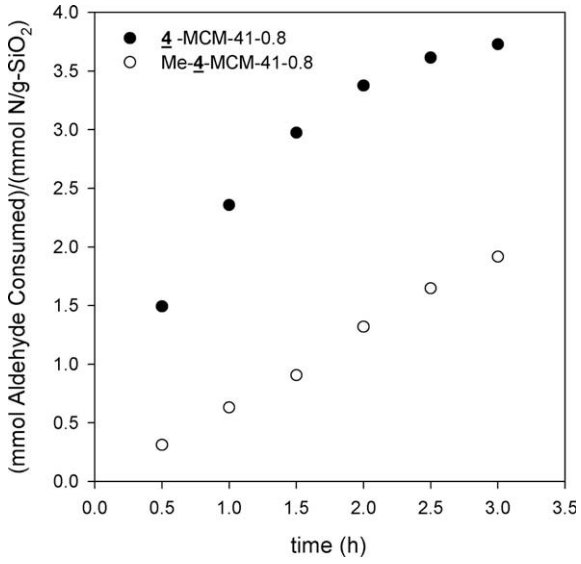


**Fig. 8.** Nitrobenzaldehyde consumption normalized by the mmol of nitrogen per gram of silica for **4**-MCM-41 and a sample of **4**-MCM-41 treated with methyltrimethoxysilane.

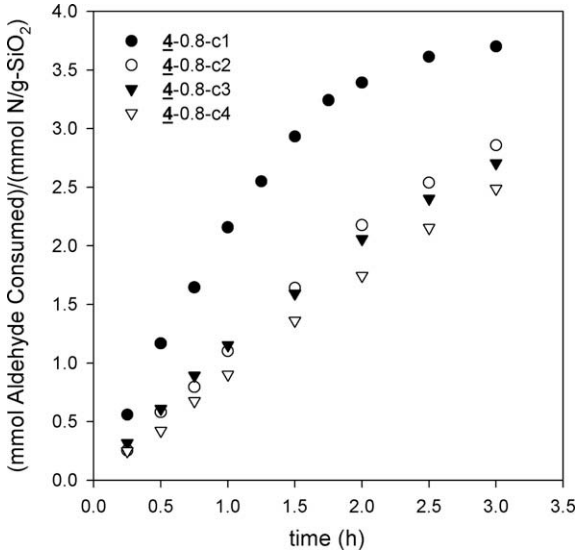


**Fig. 9.** Recycle data for **4**-MCM-41 (0.8 meq/g).

samples. A simple conclusion is that the presence of silanols are not as essential for the methylamine groups to perform this chemistry as it is the most active ligand investigated.

### 3.2.4. Catalyst stability

In order to check the stability of the materials, samples of **4** were recycled and the data are shown in Fig. 9. The reaction rate decreases for the 2nd testing cycle, but appears stable in subsequent recycle measurements. The conversion after 2 h is still higher than 50%, and a similar selectivity to nitroalcohol product was observed as in the initial run. The decrease in conversion is possibly due to the incomplete removal of absorbed species from the active sites by nitromethane and methanol. Ongoing work is investigating this issue in more detail. As a whole, the benzylamine-MCM-41 displayed relatively stable catalytic activity and selectivity.

### 3.2.5. Effect of substrate

Fig. 10 shows the conversion of nitrobenzaldehyde catalyzed by 0.8 mmol/g **4** attached on SBA-15. The total conversion is much lower than that catalyzed by *N*-benzylpropylamine-functionalized MCM-41. There are several possible explanations for the observed behavior. First, the smaller pore size of MCM-41 (3.8 nm) could lead to stronger adsorption of the reactants and perhaps lead to enhanced reaction rates. We have no direct evidence for this beyond the marked decrease in activity for the ligand supported on SBA-15 (7.8 nm). Another possibility is that due to the micropores in SBA-15, some of the grafted amines preferentially attach in/near the micropores and are thus inaccessible. This could explain some, but likely not all the decrease in activity observed. The TGA data does show a lower amine loading on SBA-15 (0.46 mmol/g silica) than expected. Finally, given the lower surface area of SBA-15, there will be statistically fewer silanol groups at a given amine loading. While we cannot eliminate one over any other, all three of these possibilities could contribute to the reduced activity observed.

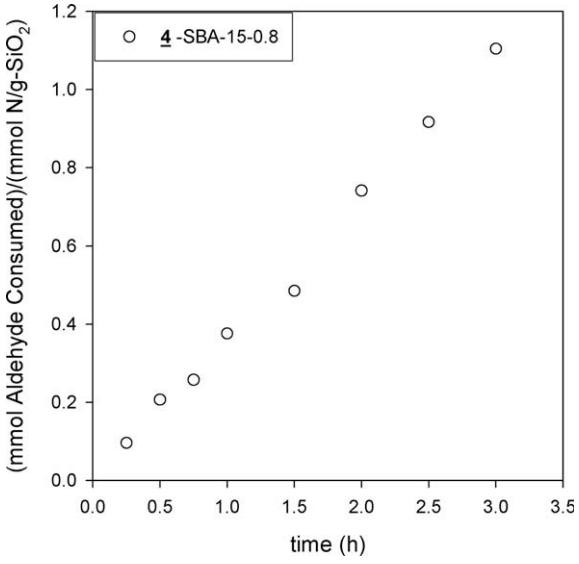


**Fig. 10.** Nitrobenzaldehyde consumption normalized by the mmol of nitrogen per gram of silica for **4**-SBA-15.

## 4. Conclusions

The effects of amine identity, structure, loading, presence of surface silanols, and the substrate topology on the Henry reaction have been investigated. Consistent with previous results, primary amines favor the formation of the alkene product, while secondary and tertiary amines favor the formation of the alcohol products. Among the secondary amines, the least sterically hindered amine (*N*-methylamine) was the most active. In nearly all samples, the capping of the silanol groups with hexamethyldisilazane dramatically decreased the activity of the materials, implying the need for cooperativity between the surface amine and silanol groups. There are also clear support effects as the benzylamine ligand was much more active when grafted to MCM-41 when compared to SBA-15.

## Acknowledgment

The authors acknowledge financial support from the National Science Foundation (CTS-0624813).

## Appendix A. Supplementary material

Supplementary data associated with this article can be found, in the online version, at doi:10.1016/j.jcat.2010.01.010.

## References

[1] M.E. Davis, Nature 417 (2002) 813–821.
[2] A. Corma, H. Garcia, Adv. Synth. Catal. 348 (2006) 1391–1412.
[3] D.M. Ford, E.E. Simanek, D.F. Shantz, Nanotechnology 16 (7) (2005) S458–S475.
[4] A.P. Wight, M.E. Davis, Chem. Rev. 102 (2002) 3589–3613.
[5] F. Hoffmann, M. Cornelius, J. Morell, M. Froba, Angew. Chem. Int. Ed. 45 (20) (2006) 3216–3251.
[6] A. Stein, Adv. Mater. 15 (2003) 763–775.
[7] K. Sakaguchi, M. Matsui, F. Mizukami, Appl. Microbiol. Biotechnol. 67 (3) (2005) 306–311.
[8] S. Yoo, J.D. Lunn, S. Gonzalez, J.A. Ristich, E.E. Simanek, D.F. Shantz, Chem. Mater. 18 (13) (2006) 2935–2942.
[9] D.R. Radu, C.Y. Lai, K. Jeftinija, E.W. Rowe, S. Jeftinija, V.S.Y. Lin, J. Am. Chem. Soc. 126 (41) (2004) 13216–13217.
[10] A. Corma, H. Garcia, Chem. Rev. 103 (2003) 4307–4365.
[11] Y. Wan, D. Zhao, Chem. Rev. 107 (7) (2007) 2821–2860.
[12] D. Astruc, F. Lu, J.R. Aranzaes, Angew. Chem. Int. Ed. 44 (2005) 7852–7872.
[13] L.M. Bronstein, Top. Curr. Chem. 226 (2003) 55–89.
[14] J.D. Holmes, D.M. Lyons, K.J. Ziegler, Chem. Eur. J. 9 (2003) 2144–2150.
[15] B.F.G. Johnson, Top. Catal. 24 (2003) 147–159.
[16] Q.Q. Wang, D.F. Shantz, J. Solid State Chem. 181 (7) (2008) 1659–1669.
[17] D. Brunel, A.C. Blanc, A. Galarneau, F. Fajula, Catal. Today 73 (1–2) (2002) 139–152.
[18] M. Alvaro, A. Corma, D. Das, V. Fornes, H. Garcia, Chem. Commun. (8) (2004) 956–957.
[19] A. Cauvel, G. Renard, D. Brunel, J. Org. Chem. 62 (3) (1997) 749–751.
[20] D. Brunel, Microporous Mesoporous Mater. 27 (2–3) (1999) 329–344.
[21] S.J.O. Julia-Christina Wasilke, R. Tom Baker, Guillermo C. Bazan, Chem. Rev. 105 (3) (2005) 1001–1020.
[22] V. Dufaud, M.E. Davis, J. Am. Chem. Soc. 125 (31) (2003) 9403–9413.
[23] D.R. Radu, C.Y. Lai, J.G. Huang, X. Shu, V.S.Y. Lin, Chem. Commun. (10) (2005) 1264–1266.
[24] Y.F. Feng, X.Y. Yang, Y. Di, Y.C. Du, Y.L. Zhang, F.S. Xiao, J. Phys. Chem. B 110 (29) (2006) 14142–14147.
[25] M.K. Kidder, P.F. Britt, Z.T. Zhang, S. Dai, A.C. Buchanan, Chem. Commun. (22) (2003) 2804–2805.
[26] R.J. Chimentao, S. Abello, F. Medina, J. Llorca, J.E. Sueiras, Y. Cesteros, P. Salagre, J. Catal. 252 (2) (2007) 249–257.
[27] Y. Kubota, Y. Nishizaki, H. Ikeya, M. Saeki, T. Hida, S. Kawazu, M. Yoshida, H. Fujii, Y. Sugi, Microporous Mesoporous Mater. 70 (1–3) (2004) 135–149.
[28] Y. Kubota, H. Ikeya, Y. Sugi, T. Yamada, T. Tatsumi, J. Mol. Catal. A – Chem. 249 (1–2) (2006) 181–190.
[29] Y. Kubota, Y. Sugi, T. Tatsumi, Catal. Surv. Asia 11 (4) (2007) 158–170.
[30] F.C. Bigi, S. Maggi, R. Mazzacani, A.G. Sartori, Stud. Surf. Sci. Catal. (2000) 130.
[31] J.D. Bass, S.L. Anderson, A. Katz, Angew. Chem. Int. Ed. 42 (42) (2003) 5219–5222.
[32] J.D. Bass, A. Katz, Chem. Mater. 15 (2003) 2757–2763.
[33] X.G. Wang, K.S.K. Lin, J.C.C. Chan, S.F. Cheng, J. Phys. Chem. B 109 (5) (2005) 1763–1769.
[34] G. Wulff, B. Heide, G. Helfmeier, J. Am. Chem. Soc. 108 (5) (1986) 1089–1091.
[35] A. Walcarius, M. Etienne, B. Lebeau, Chem. Mater. 15 (11) (2003) 2161–2173.
[36] X.G. Wang, K.S.K. Lin, J.C.C. Chan, S. Cheng, Chem. Commun. (23) (2004) 2762–2763.
[37] J.C. Hicks, R. Dabestani, A.C.I. Buchanan, C.W. Jones, Chem. Mater. 18 (2006) 5022–5032.
[38] K.K. Sharma, R.P. Buckley, T. Asefa, Langmuir 24 (24) (2008) 14306–14320.
[39] D.J. Macquarrie, R. Maggi, A. Mazzacani, G. Sartori, R. Sartorio, Appl. Catal. A – Gen. 246 (1) (2003) 183–188.
[40] S. Huh, J.W. Wiench, J.-C. Yoo, M. Pruski, V.S.Y. Lin, Chem. Mater. 15 (2003) 4247–4256.
[41] M.H. Lim, A. Stein, Chem. Mater. 11 (1999) 3285–3295.
[42] M.W. McKittrick, C.W. Jones, Chem. Mater. 15 (2003) 1132–1139.
[43] T. Yokoi, H. Yoshitake, T. Yamada, Y. Kubota, T. Tatsumi, J. Mater. Chem. 16 (12) (2006) 1125–1135.
[44] J.C. Hicks, C.W. Jones, Langmuir 21 (2006) 2676–2681.
[45] X.H. Lin, G.K. Chuah, S. Jaenicke, J. Mol. Catal. A – Chem. 150 (1–2) (1999) 287–294.
[46] S. Jaenicke, G.K. Chuah, X.H. Lin, X.C. Hu, Microporous Mesoporous Mater. 35–36 (2000) 143–153.
[47] K. Shimizu, H. Suzuki, E. Hayashi, T. Kodama, Y. Tsuchiya, H. Hagiwara, Y. Kitayama, Chem. Commun. (10) (2002) 1068–1069.
[48] K.-I. Shimizu, E. Hayashi, T. Inokuchi, T. Kodama, H. Hagiwara, Y. Kitayama, Tetrahedron Lett. 43 (2002).
[49] J.D. Bass, A. Katz, Chem. Mater. 18 (6) (2006) 1611–1620.
[50] J.D. Bass, A. Solovyov, A.J. Pascall, A. Katz, J. Am. Chem. Soc. 128 (11) (2006) 3737–3747.
[51] K.K. Sharma, T. Asefa, Angew. Chem. Int. Ed. 46 (16) (2007) 2879–2882.
[52] A. Anan, R. Vathyam, K.K. Sharma, T. Asefa, Catal. Lett. 126 (1–2) (2008) 142–148.
[53] H.T. Chen, S. Huh, J.W. Wiench, M. Pruski, V.S.Y. Lin, J. Am. Chem. Soc. 127 (38) (2005) 13305–13311.
[54] P. Banet, N. Marcotte, D.A. Lemer, D. Brunel, Langmuir 24 (16) (2008) 9030–9037.
[55] R.K. Zeidan, S.-J. Hwang, M.E. Davis, Angew. Chem. Int. Ed. 45 (2006) 6332–6335.
[56] R.K. Zeidan, M.E. Davis, J. Catal. 247 (2) (2007) 379–382.
[57] E.L. Margelefsky, A. Bendjeriou, R.K. Zeidan, V. Dufaud, M.E. Davis, J. Am. Chem. Soc. 130 (2008) 13442–13449.
[58] E.L. Margelefsky, R.K. Zeidan, V. Dufaud, M.E. Davis, J. Am. Chem. Soc. 129 (2007) 13691–13697.
[59] S. Huh, H.T. Chen, J.W. Wiench, M. Pruski, V.S.Y. Lin, J. Am. Chem. Soc. 126 (4) (2004) 1010–1011.
[60] S. Huh, H.T. Chen, J.W. Wiench, M. Pruski, V.S.Y. Lin, Angew. Chem. Int. Ed. 44 (12) (2005) 1826–1830.
[61] E.L. Margelefsky, R.K. Zeidan, M.E. Davis, Chem. Soc. Rev. 37 (6) (2008) 1118–1126.
[62] K.J. Edler, J.W. White, Chem. Mater. 9 (5) (1997) 1226–1233.
[63] D.Y. Zhao, Q.S. Huo, J.L. Feng, B.F. Chmelka, G.D. Stucky, J. Am. Chem. Soc. 120 (24) (1998) 6024–6036.
[64] M. Jaroniec, M. Kruk, J.P. Olivier, Langmuir 15 (16) (1999) 5410–5413.
[65] F. Rouquerol, J. Roquerol, K. Sing, Adsorption by Powders and Porous Solids, Academic, San Diego, 1999.
[66] M. Kruk, M. Jaroniec, A. Sayari, Langmuir 13 (23) (1997) 6267–6273.
[67] Q. Wang, E. Jordan, D.F. Shantz, J. Phys. Chem. C 113 (42) (2009) 18142–18151.
[68] S.L. Hruby, B.H. Shanks, J. Catal. 263 (2009) 181–188.